Available online at www.sciencedirect.com
SCIENCE DIRECT®
Physics of the Earth and Planetary Interiors 153 (2005) 61–73
PHYSICS OF THE EARTH AND PLANETARY INTERIORS
www.elsevier.com/locate/pepi

A paleomagnetic power spectrum

Catherine Constable*, Catherine Johnson[1]

Green Institute of Geophysics and Planetary Physics, Scripps Institution of Oceanography, University of California at San Diego, 9500 Gilman Drive La Jolla, La Jolla, CA 92093-0225, USA

Received 22 November 2004; received in revised form 29 March 2005; accepted 30 March 2005

Abstract

We construct a power spectrum of geomagnetic dipole moment variations or their proxies that spans the period range from some tens of million down to about 100 years. Empirical estimates of the spectrum are derived from the magnetostratigraphic time scale, from marine sediment relative paleointensity records, and from a time varying paleomagnetic field model for the past 7 kyr. The spectrum has the most power at long periods, reflecting the influence of geomagnetic reversals and in general decreases with increasing frequency (decreasing period). The empirical spectrum is compared with predictions from simple models. Discrepancies between the observed and predicted spectra are discussed in the context of: (i) changes in reversal rate, (ii) overall average reversal rate, (iii) cryptochrons, (iv) the time taken for a reversal to occur, and (v) long term paleosecular variations and average estimates of the field strength and variance from other sources.

Keywords: Geomagnetism; Paleomagnetism; Paleomagnetic power spectrum; Paleosecular variations

1. Introduction

The geomagnetic field exhibits a rich array of temporal variation attributable to processes both within and external to Earth (e.g. Merrill et al., 1996). Today, paleomagnetic data are used to analyze geomagnetic field variations on time scales ranging from hundreds to billions of years. Yet there remains much that is poorly documented about geomagnetic field variations, including the nature of the paleomagnetic spectrum. Still unanswered is the basic question of how long one needs to average the geomagnetic field in order to uncover a stable time-averaged field, assuming that such a thing exists. Paleomagnetic power spectra can help with this question and also pave the way to extend existing statistical models for paleosecular variation (PSV) to include temporal covariance. Such models and the distribution of power over the full range of frequencies represent important statistical properties that can be used for comparison with the burgeoning output of geodynamo simulations (e.g. McMillan et al., 2001; Kono and Roberts, 2002; Bouligand et al., 2005).

Spectral analysis is widely used throughout the physical and Earth sciences as a tool to identify the frequency content of signals, usually with the hope of categorizing specific behaviors and their physical causes. Paleomagnetism is no exception, and there have been numerous analyses of time series of observations. Substantial effort has been devoted to seeking or debunking evidence for periodicities in changes in reversal rate (see e.g., Constable, 2000). A plethora of studies deal with periodic variations at or near timescales characteristic of

* Corresponding author. Tel.: +1 858 534 3183; fax: +1 858 534 8090.
E-mail addresses: cconstable@ucsd.edu (C. Constable); cljohnson@ucsd.edu (C. Johnson).
[1] Tel.: +1 858 822 4077; fax: +1 858 534 5332.

0031-9201/$ – see front matter © 2005 Elsevier B.V. All rights reserved.
doi:10.1016/j.pepi.2005.03.015

the changes in eccentricity, obliquity, and precession parameters associated with Earth's orbit, beginning with the suggestion by Wollin et al. (1978) and still an active source of controversy (e.g. Channell et al., 1998; Guyodo et al., 2000; Yamazaki and Oda, 2002; Roberts et al., 2003). At shorter time scales lake sediment records have repeatedly been analyzed in the hope of uncovering characteristic time scales of variations and evidence for long term westward (or eastward) drift (e.g., Denham, 1975; Barton and McElhinny, 1982). However, the heterogeneous nature of paleomagnetic data has so far made it difficult to establish a spectrum that spans the full range of paleomagnetic temporal variations. Events like reversals (often treated as point processes) are hardly commensurate with the directional variations of the magnetic field that are most readily recovered from lake sediments. During the past 20 years a huge number of measurements of relative geomagnetic paleointensity variations have been derived from marine sediments, with temporal spans ranging from a few tens of kyr to several millions of years. Many of these have been subjected to individual spectral analyses and the records have been stacked and averaged to provide estimates of the global dipole moment for the past 800 kyr (Guyodo and Valet, 1999), but these have yet to be fully integrated with either shorter or longer term spectral estimates.

We present a power spectrum for the geomagnetic dipole moment for the time interval 0–160 Ma. The spectrum is constructed from an array of paleomagnetic datasets: at the very longest periods we use the magnetostratigraphic time scale constructed from marine magnetic anomalies; between 10^6 and 10^3 years the records of choice are marine sediments; and from 10^3 to 10^2 year periods we draw on a time-varying geomagnetic field model constructed from lake sediments, young lava flows, and archeomagnetic observations. We compare direct estimates from data with those acquired from simplified models concerning reversal rates, and assess the internal consistency of our results using the time-averaged field and its variance inferred from absolute measurements of geomagnetic paleointensity for the same time interval.

2. Spectral analysis: the dipole moment and choice of method

Our goal is to analyze how variations in the strength of the paleomagnetic field are distributed as a function of frequency. The parameter which we choose to represent magnetic field strength is the geomagnetic dipole moment or a proxy form for times where we cannot obtain a direct estimate. The choice of dipole moment (as opposed to some other geomagnetic field parameter) is motivated in large part by the dominance of the geocentric axial dipole when the field is averaged over long time intervals: the strength of the axial dipole is a globally representative feature of the field, and may be related to the amount of energy required by the geodynamo or perhaps to the frequency of occurrence of geomagnetic reversals (e.g., Cox, 1969; Prévot et al., 1990; Constable et al., 1998). Although it is possible that other properties of the field (such as non-dipole field contributions) directly represent particular physical processes controlling the secular variation and may interact with the dipole part of the field, resolving such variations in paleomagnetic time series that extend back tens of millions of years before present remains questionable. One might also wonder whether directional variation can give a better representation of field variability, thereby avoiding some of the difficulties inherent in measuring paleointensity. But at low frequencies the dominance of the axial dipole means there is very little power in directional variations except during geomagnetic reversals: in contrast, large variations in dipole strength are not necessarily associated with reversals.

A basic requirement for spectral analysis is a time series of observations. In constructing a paleomagnetic power spectrum we face several challenges. There is no single record that covers the time span of interest, so we must combine different kinds of records. The relative paleointensity records from sediments not only lack an absolute scale, but are usually unevenly sampled in time so that some stable interpolation scheme is required before using the standard analysis techniques. It is likely that some records record a smoothed version of the geomagnetic signal because of low sedimentation rates, while in others it may be necessary to consider the possibility of aliasing. Non-geomagnetic signals may be inadvertently interpreted as arising from geomagnetic variations with time. These issues are considered in more detail in Section 3 for the specific records we have analyzed.

Power spectral analysis is usually carried out using variants of one of the following well-known techniques: (1) direct spectral estimation using extensions and improvements to the time-honored periodogram method introduced by Schuster (1998); (2) the autocovariance method pioneered by Blackman and Tukey (1958); (3) parametric modeling schemes like the maximum entropy method based on a discrete autoregressive process (Burg, 1967).

It would be tedious to review here the vast array of analyses conducted on individual paleomagnetic records and the relative merits of these techniques used for particular studies. Instead we note that we consider (3) inap-

propriate for the geomagnetic field because it is unclear what form of parametric model would apply. Method (2) is widely used in paleomagnetic and paleoclimate studies because of the ready availability of the Analyseries software package Paillard et al. (1996). The Blackman–Tukey method exploits the fact that the autocovariance and power spectral density of a stochastic process form a Fourier transform pair. The autocovariance is estimated first, then windowed and Fourier transformed to provide a spectral estimate. The algorithm, often termed an indirect spectral estimate, reflects the fact that before the advent of the fast Fourier transform in the mid-1960s direct spectral estimation could be computationally challenging. The method generally provides poor resolution in the spectral domain compared with modern direct methods.

Our preferred technique is multi-taper direct spectral estimation: tapering of the data series and averaging of independent spectral estimates are commonly used to offset the twin evils of bias and variance in spectral estimates (e.g., Percival and Walden, 1993). The multi-taper method uses mutually orthogonal members of families of tapers, which have approximately uncorrelated spectral estimates. This allows one to exploit the full length of the data record in each independent spectral estimate that contributes to the average, thereby obtaining the largest available frequency range. Two families of tapers are in common use. The prolate spheroidal wave functions concentrate the spectral energy within a prespecified frequency bandwidth (Thomson, 1982), and can be used in multi-taper spectral estimates that are resistant to broadband spectral leakage. A completely different family of tapers minimize local bias (Riedel and Sidorenko, 1995) and are closely approximated by sine functions. The spectral estimation method based on these sine multi-tapers, which we adopt here, has the advantage that it is locally adaptive and one can readily adjust the amount of spectral averaging to reflect the amount of detail present in the spectrum at different frequencies. If needed, pre-whitening can be used for protection against the broadband spectral bias typically associated with a sharp fall-off in the spectrum. We explored prewhitening in our analyses, but did not find it necessary.

The locally adaptive method means that both the resolution and the error vary in the frequency domain. In the multi-taper spectral code used in this work, the errors are computed as one standard error of the averaged spectrum at the specified frequency (Parker, personal communication, 2005). When k multi-tapers are used in the estimate the frequency resolution is kf_N/N_f with f_N the Nyquist frequency, and N_f the number of frequencies estimated. The adaptive part of the procedure is the optimal choice of k. Riedel and Sidorenko (1995) give an asymptotic result for minimizing the local loss (bias squared plus variance) of:

$$k_{\mathrm{opt}} = \left[\frac{12S(f)N^2}{S''(f)}\right]^{2/5}.$$

where S'' is determined from a quadratic fit to a pilot estimate of the local power spectral density, but the above expression must be modified to restrict the rate of growth of number of tapers near regions where S'' vanishes. The spectra from the individual sine tapers are averaged, with parabolic weighting that tapers to zero beyond the kth spectral estimate. This weighting scheme ensures a smooth spectrum as the number of tapers changes with frequency.

All of the techniques discussed suppose that the underlying process is stationary, an assumption that could be called into question for the geomagnetic field and the processes by which it is recorded. Changes in spectral content with time can be evaluated, by studying segmented sections of the paleomagnetic record.

This is not the first attempt to assess the paleomagnetic power spectrum. Barton (1983) provided a thorough tutorial on using the periodogram and maximum entropy methods for the analysis of paleomagnetic directional data, noting the many potential pitfalls associated with spectral analysis. He also applied the periodogram analysis (Barton, 1982) in an attempt to integrate power spectra from sediment records with those from magnetic observatories for periods ranging from less than a year to 10^5 years. Courtillot and Le Mouël (1988) reviewed geomagnetic field variations on time scales from seconds to millions of years and merged Barton's result with other spectral estimates to provide a schematic power spectrum for an extended time scale. They debated whether this is compatible with a $1/f^2$ spectrum, and concluded that it was too early to make such an inference. The purpose of this work is to exploit improvements in spectral estimation techniques offered by the multi-taper method, together with some vastly improved paleomagnetic intensity records, and use them to update the paleomagnetic part of the spectrum.

3. The paleospectrum

3.1. The magnetostratigraphic spectrum

3.1.1. A model

In the absence of reliable measurements of very long (greater than a few million years) time series of paleointensity variations, we use a magnetostratigraphic

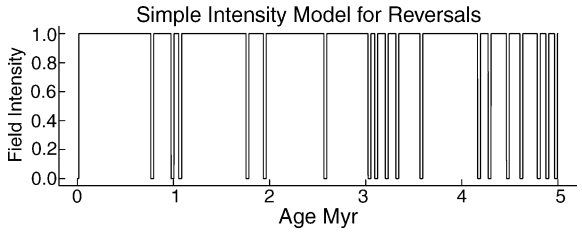

Fig. 1. Sample of a field intensity record simulated using the simple model described in the text. Reversals are treated as a Poisson process with rate λ. During reversals the field strength drops to zero for a time period δ before returning to full strength.

timescale and a simplistic statistical model which supposes that field strength is constant except during finite intervals when the field is reversing. During the reversal the dipole moment is diminished, but also constant. The reversal model is that of a Poisson process, one in which at any given instant the probability per unit time of a transition to the opposite polarity state is constant. (Constable et al., 1998) derived a theoretical estimate for the spectrum of this kind of boxcar variation under the assumption that the reversal rate is constant. A hypothetical sample of the reversal model with unit amplitude is shown in Fig. 1.

The dipole moment, $m(t)$, is constant, here taken to be A, outside the transition intervals. During a transition, m drops to zero and stays there for a period of time δ, then returns to A. λ is the rate parameter of a Poisson process. In the Appendix of Constable et al. (1998), it is shown that such a process is characterized by a mean dipole moment of:

$$E(m(t)) = M = A\mathrm{e}^{-\lambda\delta}. \tag{1}$$

The autocovariance for the process is

$$R_m(t) = \begin{cases} A^2[\mathrm{e}^{-\lambda(|t|+\delta)} - \mathrm{e}^{-2\lambda\delta}], & \text{if } |t| \le \delta; \\ 0, & |t| > \delta, \end{cases} \tag{2}$$

and the theoretical power spectrum is given by the Fourier transform of the autocovariance of the process:

$$\begin{aligned} S_m(f) &= 2\int_{-\infty}^{\infty} \mathrm{d}t\, \mathrm{e}^{-2\pi i f t} R_m(t) \\ &= \frac{4A^2\lambda\, \mathrm{e}^{-\lambda\delta}}{\lambda^2 + 4\pi^2 f^2} \\ &\quad \times \left(1 - \mathrm{e}^{-\lambda\delta}\left[\cos 2\pi f\delta + \frac{\lambda\, \sin\, 2\pi f\delta}{2\pi f}\right]\right). \end{aligned} \tag{3}$$

Under this model, the time required to acquire a reliable average for the dipole moment and the average value itself depend on both the reversal rate and the typical duration of reversals. Fig. 2a shows the dependence of the normalized average field value ($\mu = M/A$), the standard deviation ($s = \sqrt{R_m(0)}/A$), and its normalized value ($\hat{s} = s/M$) on the product $\lambda\delta$, the fraction of the time that the model field spends in a transitional state ($\hat{s}$ is of interest because in paleomagnetism it is often only possible to derive relative intensity variations). Fig. 2b shows the corresponding relationship between average moment and $\hat{s}$ under this model.

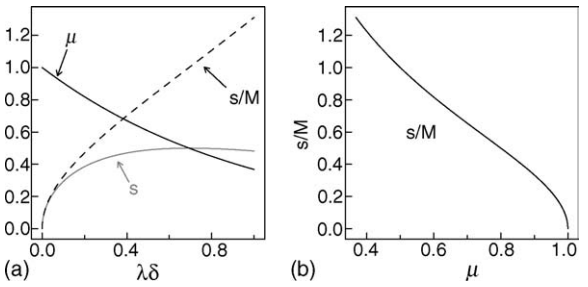

Fig. 2. (a) Dependence of mean field and its normalized standard deviation on the fraction of time the field spends in a transitional state. (b) Relationship between the normalized standard deviation and the normalized mean field.

To relate this model to actual field behavior we attempt to place some bounds on plausible values for $\lambda\delta$. Over the past 160 Ma, the field has reversed 280 times, but the rate is far from uniform, with typical estimates ranging from zero during the almost 40 Myr long Cretaceous normal superchron to about 4 Myr^{-1} near the beginning and end of the 160 Myr period. Point-wise 95% confidence bounds on the rates for a Poisson process range up to 20 Myr^{-1} (Constable, 2000). Supposing the average reversal rate to be 2 Myr^{-1} and the time for a reversal about 10 kyr, we might expect the appropriate value of $\lambda\delta$ to be around 0.02. This is not inconsistent with some estimates of the time the field spends in a transitional state. However, one should keep in mind that average reversal rates more than twice as high have been inferred during some time intervals over the past 160 Myr, and if the short cryptochrons (Cande and Kent, 1992, 1995) that are believed to represent large intensity variations, geomagnetic excursions, or very short polarity intervals were also included the rate would rise higher still. Estimates of the time taken for the field to reverse have also been highly variable (for review see e.g., Constable, 2003) with end members ranging from about 100 years to as high as about 20 kyr when intensity variations are the criterion used to identify the reversal time. Thus a conservative view might put an upper bound of 0.4 on $\lambda\delta$ for the past 160 Myr, though it remains a possibility that over short time intervals or at times in the more distant past higher values might be relevant.

A field with $\lambda\delta = 0.4$ might be considered rather unstable by today's standards, but it is also worth noting that the simple model here has quite different behavior for larger values of $\lambda\delta$. The probability of individual reversals merging to form longer intervals of zero dipole moment increases, and the variance starts to decrease after attaining its maximum value at $\lambda\delta = \ln 2$. A field that is stable with dipole moment of A with intermittent reversals is gradually replaced by a zero moment field with an occasional short excursion to dipole moment A. One might think of this as an intermittent dynamo that occasionally turns on. During the Cretaceous normal superchron from 83 to 124 Ma there are no recorded geomagnetic reversals: one interpretation would be that $\lambda\delta = 0$ at this time. These results may seem trivial, but the simple model serves to highlight the need for adequate temporal sampling to define the mean and variance of paleomagnetic field intensity.

Although the mean and overall variance are completely determined by the product $\lambda\delta$ the spectrum varies independently for each parameter. For a fixed reversal rate the spectrum described by Eq. 3 is essentially constant at low frequency and falls off approximately as the inverse square of the frequency above a critical value determined by the characteristic reversal transition length. Fig. 3a shows how the transition length influences the long period part of the spectrum for a reversal rate fixed at 5 Myr^{-1}. As the transition length increases there is more energy in the long period field variations. In Fig. 3b we find that fixing the transition length pegs the corner frequency at which the power begins to drop off: but the power level across the whole frequency band increases with the reversal rate, until reversal rate becomes so high that adjacent reversals begin to merge with one another.

The average value for the dipole moment has no influence on the spectrum, what matters is the difference in amplitude between the stable state and the reversing state which contributes to the variance of the process. The actual geomagnetic spectrum will differ from this model because of changes in reversal rate, any fluctuations in paleointensity, and lack of uniformity in the time taken for individual reversals. Constable et al. (1998) note that a more complicated shape for the transition to low intensity can be easily accommodated in this model by convolving the step with a shape factor $g(t)$. Eq. (3) for $S(f)$ is then modified to:

$$\tilde{S}(f) = |\hat{g}|^2 S(f)$$

where $\hat{g}$ is the Fourier transform of g.

3.1.2. A spectrum based on the real time scale

In this section, we investigate the limitations imposed by assuming a constant reversal rate in the model described above, by calculating the power spectrum for the real magnetostratigraphic time scale on the time interval 0–160 Ma. We use the scale of Cande and Kent (1995) for 0–84 Ma, merged with that of Harland et al. (1990) for the older part, and refer to this record as CK95. In Fig. 4, we show the power spectrum estimated using Riedel and Siderenko's minimum bias multi-taper adaptive method for a dipole moment that drops to zero every time the field reverses and remains there for a fixed period of 10 kyr (blue), 20 kyr (pink), or 30 kyr (black), corresponding to fields that are transitional roughly 1.8, 3.6, or 5.4% of the time when averaged over the whole time span. The theoretical spectrum predicted by Eq. 3 for a constant rate process of $2Myr^{-1}$ is given in green, and agrees well with the corresponding empirical curve for 1.8% transitional field for frequencies higher than $0.1Myr^{-1}$.

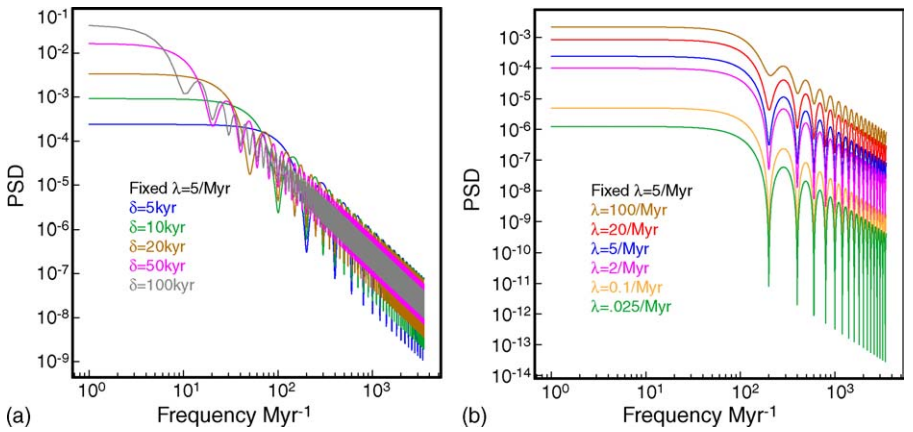

Fig. 3. Variations in power spectral density (PSD) for the simple model of Poisson intensity variations illustrated in Fig. 1. (a) Fixed reversal rate, λ; variable transition lengths, δ. (b) Fixed transition length, δ; variable reversal rate.

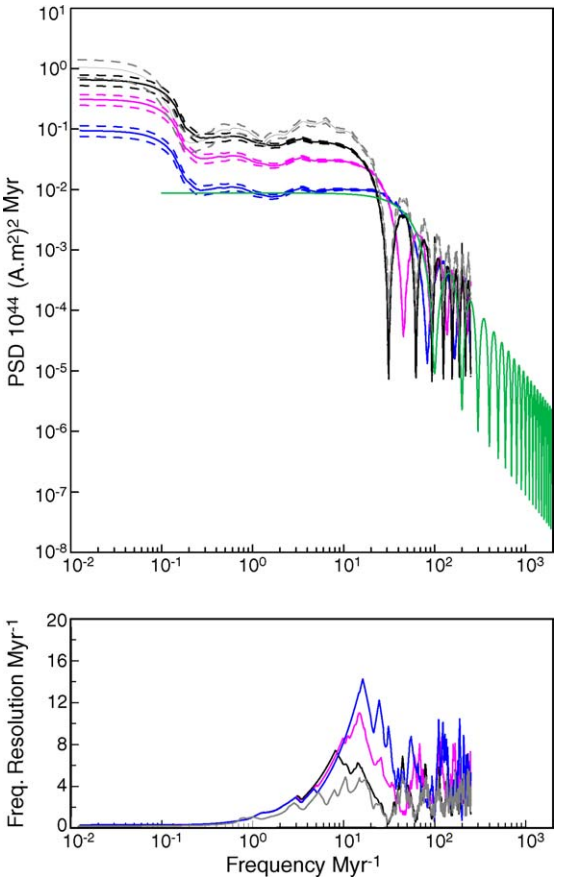

Fig. 4. Power spectrum estimated for reversal times of the past 160 Ma (containing 280 reversals) using Riedel and Sidorenko (1995) minimum bias mutitaper method (upper panel). Blue, pink and black curves give estimates from CK95 assuming $\delta = 10, 20$ or 30 kyr, respectively, for the interval 0–160 Ma. Gray curve is for CK95cc: the time interval is 0–83 Ma with $\delta = 30$ kyr, and cryptochrons are included. Dashed lines give one standard error estimates. Green curve is the theoretical spectrum predicted by Eq. (3) for $\lambda\delta = 0.02$, corresponding to the average reversal rate and length for the blue curve. Lower panel shows the frequency resolution for the corresponding spectral estimates.

The differences at longer period arise from changes in the long-term geomagnetic reversal rate; we verified that it is straightforward to reproduce the green curve empirically by simulation from a Poisson process with constant rate and appropriate parameters. As demonstrated in Fig. 3a, a larger overall variance is associated with longer reversal intervals, and the increase in δ also decreases the corner frequency. We investigated the effects of non-stationarity in the record, by estimating the spectrum independently for 40 Myr sections of the record. The primary effect that we noted is that the variance scales with the average reversal rate within each section, again reflecting the long period changes in reversal rate.

Cande and Kent (1995) were careful to produce a timescale that had uniform temporal resolution, despite the variable nature of the magnetic anomaly records from which it is constructed. However, they also noted the presence of cryptochrons which are particularly prevalent in the better resolved parts of the record, one of which is Chron 12R (extending from 33.05 to 30.915 Ma) in the early Oligocene. Cryptochrons are ambiguous parts of the anomaly record which might be very short polarity chrons, long term fluctuations in paleointensity, or geomagnetic excursions. We analyzed the record for the interval 0–84 Ma with the cryptochrons included, and $\delta = 30$ kyr (gray curve, Fig. 4), treating each cryptochron like a full reversal in our model. We designate this intensity record CK95cc, to distinguish it from the longer and more uniform CK95. The spectrum shows more structure which partly reflects the uneven resolution of the cryptochron time scale, but the higher overall power is more likely to be representative of the energy in the magnetic field in this frequency band. As there are 292 events in the 83 Myr cryptochron scale, this would correspond to a field that is transitional 10.5% of the time.

The magnetostratigraphic spectrum is scaled to provide absolute estimates of dipole moment using the average value of virtual dipole moments derived from absolute paleointensity estimates for 0–160 Ma. A current estimate for the mean is given by Tauxe (2005) as $4.5 \pm 1.8 \times 10^{22}$ Am^2, where the 1.8 is not a standard error in the mean, but an estimate of the standard deviation of the distribution of moments. If we accept the model parameters used for the black curve in Fig. 4, we expect the mean to be $M = 0.947$ A and the variance $R_m(0) = 0.049$ A^2. Scaling accordingly, we find that for CK95 $A = 4.75 \times 10^{22}$ Am^2 and the associated standard deviation calculated for such a model is 1.05×10^{22} Am^2. For the cryptochron scale, CK95cc, we find $A = 5.00 \times 10^{22}$ Am^2 and standard deviation calculated for such a model is 1.5×10^{22} Am^2. The lower overall variance estimate compared with the paleomagnetic data should be expected from the fact that our simple model neglects all intensity variations apart from the abrupt drop associated with a reversal. In Section 4, when we merge this low frequency spectrum with those obtained from marine sediments, we see that model parameters corresponding to $\delta = 0.03$ Myr provide a fit consistent with other observations.

3.2. Relative geomagnetic intensity variations from marine sediments

Relative paleointensity records from sediments can provide spectral estimates at periods shorter than those

Table 1
Relative paleointensity records used in spectral analyses

Record	Site location	Time interval (Ma)	Average sedimentation rate (cm kyr^{-1})	Interpolation interval (kyr)	Scaling factor
522[a]	26°S, 5°W	29.4–34.7	0.5–1	4	3.5545×10^{22}
848/851/852[b]	2°N, 110°W	0–4	<2.5	2	1.0045×10^{22}
983[c]	60.4°N, 23.6°W	0–1	10.4	0.1	10.8766×10^{22}
984[d]	61.4°N, 24.1°W	0–0.5	12.6	0.1	11.194×10^{22}
Sint-800	Multiple	Variable	Variable	1	–

[a] (Constable et al., 1998).
[b] (Valet and Meynadier, 1993).
[c] (Channell, 1999).
[d] (Guyodo and Valet, 1999).

available from the reversal timescale. The frequency content of such spectra is influenced by the record length and the sediment accumulation rate. We investigate four individual paleointensity records: two of length 4–5 Myr with mean sedimentation rates 1–2.5 cm kyr^{-1} (Valet and Meynadier, 1993; Constable et al., 1998), and two of length 0.5–1 Myr with mean sedimentation rates of 10.40–12.6 cm kyr^{-1} (Channell, 1999). The longer records overlap the spectrum from the reversal record; the higher sedimentation records overlap the spectrum obtained from 0 to 7 kyr global model for the dipole moment (Korte and Constable, 2005). We also examine a global paleointensity stack, Sint-800, spanning the last 800 kyr (Guyodo and Valet, 1999). In order to compare data from geographically distinct locations we assume that the reported paleointensity reflects field (not lithological) changes, and we take the relative paleointensity records to be a proxy for the dipole moment. Individual paleointensity records are scaled to correspond to a mean virtual axial dipole moment (VADM) of 4.2×10^{22} Am^2—the average value for the 0–4 Myr record of Valet and Meynadier (1993), and not inconsistent with Tauxe (2005). Locations, mean sedimentation rates, the time interval spanned by each record, and the normalization applied to scale the mean paleointensity to the mean VADM are provided in Table 1.

Power spectral density (PSD) estimates are made for each scaled relative paleointensity record again using the Riedel and Sidorenko (1995) minimum bias adaptive multi-taper method. Temporal sampling within each individual record is variable, due to data gaps and changes in sedimentation rate within a core. In each case, we accepted the age scales assigned to the published data set. We use Akima (1970) splines to interpolate onto an even sampling interval. The sampling interval is chosen such that, where possible, we preserve the frequency content of the record corresponding to the greatest sedimentation rate, but avoid excessive interpolation across data gaps (see Table 1). The spectral resolution achievable will depend on the overall record length, the sedimentation rate and how much it fluctuates throughout the record, the quality of the age constraints used to transform depth to age, and the sampling interval at which measurements are made. It can be difficult to evaluate the resulting age uncertainty, which will be quite variable among our different records. McMillan et al. (2004) discuss these issues at some length in the context of the cores that collectively make up the Sint-800 record and conclude that modest errors in the dating of tie points can significantly degrade the coherence among coeval records. This results from the increased spectral bias and loss of resolution in individual spectra compared with those that could be obtained with perfect age scales and infinitely dense sampling, and is especially pronounced at high frequency.

The time series and corresponding spectra for our longer records are shown in Fig. 5. The longest record is that from the Deep Sea Drilling Project Leg 73, Site 522, currently located at 26°S, and at 33°S at the time the sediments were deposited (Hartl et al., 1993). The age-depth model was developed by Tauxe (1997) using linear interpolation between tie points to reversals in the marine magnetic anomaly timescale of Cande and Kent (1995), and reflects a steady change in sedimentation rate from about 10 to 5 m Myr^{-1}. The sampling interval ranged from 4 to 8 kyr. As there are significant data gaps in the younger part of the record we use the lower part of this core, spanning 5 Myr and 9 polarity intervals (Table 1 and Fig. 5). The second record, that of Valet and Meynadier (1993), hereafter VM93, comprises several cores from sites 848, 851 and 852 of ODP Leg 138 and spans the last 4 Myr. VM93 state that the time-depth correlation is based on detailed analyses of approximately 25 kyr density variations, that reflect carbonate content and can be tuned to the insolation curve at

65°N (Shackleton et al. (1995)). The temporal sampling interval in VM93 increases with age from about 0.9 to about 3.2 kyr. The spline interpolation across data gaps occurring at 0.59 and 3.34 Myr was inspected visually. Spectra calculated for the full 0–4 Ma record showed no significant difference from reduced-length time series that excluded these data gaps, and so we retained the complete VM93 record. The adaptive process introduces a variable resolution and error in the frequency domain, and these are shown in Fig. 5 to aid interpretation of the spectra. The 2 kyr (4 kyr) interpolation of VM93 (522) corresponds to a Nyquist frequency of 250 Myr^{-1} (125 Myr^{-1}). Spectra for both records are red (more power at long periods), as expected. The spectrum for 522 shows increased power centered at about 8 Myr^{-1}, previously reported to result from dips in paleointensity, possibly associated with cryptochrons (Hartl et al., 1993; Constable et al., 1998). The peak is significant compared with uncertainties in the spectral estimates, and is resolved in frequency, but as noted by Constable et al. (1998) its presence is dependent on including Chron 12R in the analysis. This peak is not seen in the VM93 record, which shows a smooth increase in power with decreasing frequency, likely reflecting the long-period sawtooth nature of the record. The frequency resolution decreases by about a factor of 3 for periods shorter than 20 kyr in VM93. In addition to the full spectrum of VM93 shown in Fig. 5 we investigated spectra derived from 1 Myr subsections. The effect of decreasing sediment with age (and resulting filtering of the signal) is apparent in decreased power at frequencies higher than 100 Myr^{-1} in the early part of the record.

Higher frequency estimates of the PSD are made using paleointensity records from ODP sites 983 and 984 (Channell, 1999) that come from drift sediments in the Iceland Basin. These records span the last 1.2 and 0.5 Myr respectively, and have sediment accumulation rates about an order of magnitude higher than in 522 and VM93. Age models for each site were derived by correlation of oxygen isotope data to a reference curve, and linear interpolation between individual tie points (Channell et al., 1998). For 984 the 11 tie points extend to isotopic stage 12 (about 450 ka) and are spaced about 50 kyr apart, while for 983 there are 35 tie points to isotopic stage 18 (about 650 ka), which when extrapolated give an age of 779 kyr for the Brunhes–Matuyama boundary. Due to rounding in the reported ages in the digital data file, we were unable to use the oldest 200 kyr of the 983 record. A data gap of 3.8 kyr occurs at about 845 ka in 983—again we carefully checked the spline interpolation and resulting spectra to ensure the interpolation did not introduce overshoots and spectral leakage. Spectral estimates are reported for 0–1 and 0–0.5 Ma for 983 and 984, respectively (Fig. 6). Shown on a log-linear plot the spectra for 983 and 984 appear to diverge, however, closer inspection shows that they are indistinguishable over the frequency band 40–200 Myr^{-1}, corresponding to periods of 5–25 kyr. At periods longer than 25 kyr, the power spectral estimates for 983 are about 1.5 times those of 983. Both spectra decrease smoothly with frequency. Again we investigated the robustness of these spectra by looking at sequential and parallel 0.1 Ma sections. The averages from these results are essentially indistinguishable from the multi-taper result for the whole time interval. The rather minor differences between the 983 and 984 spectra at high frequency may reflect the

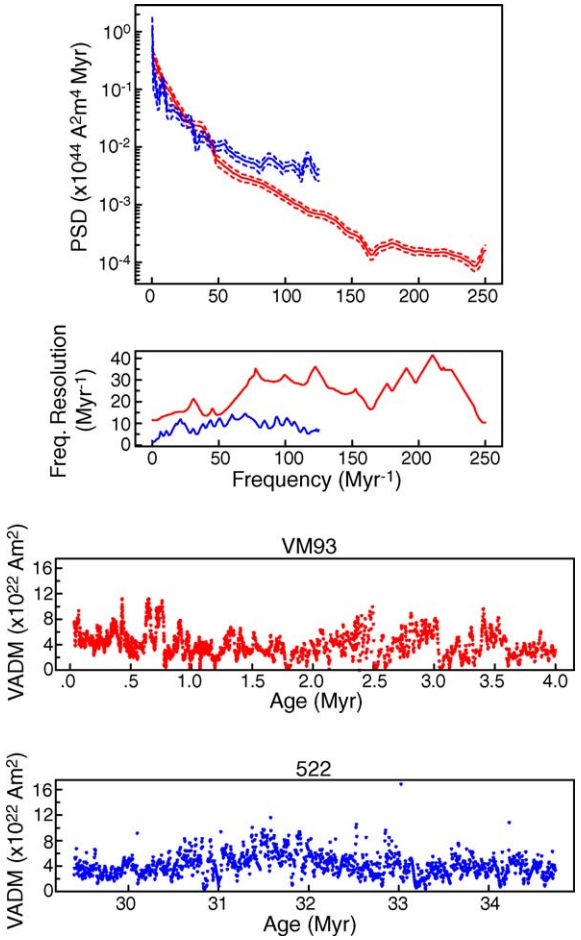

Fig. 5. Records of dipole moment (lower figures) and corresponding power spectral density estimates (upper figure) for records 522 (blue) and VM93 (red). The scaling of relative paleointensity to dipole moment is described in the text. The mean (solid line) and upper and lower $1-\sigma$ error bounds on the spectral estimates are shown. Note the log-linear scaling. The frequency resolution of the spectral estimates is indicated.

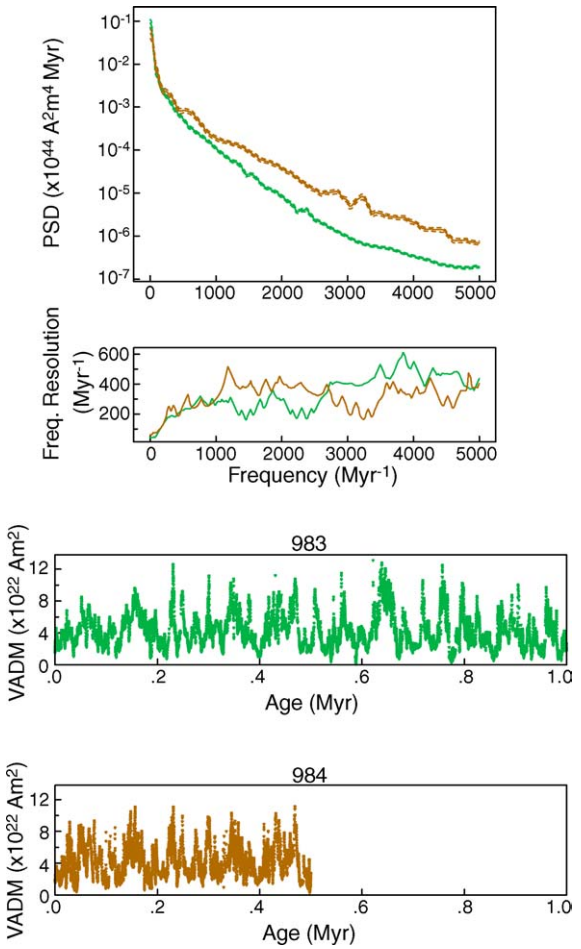

Fig. 6. Records of dipole moment (lower figures) and the corresponding power spectral density estimates (upper figure) with their frequency resolution for records 983 (green) and 984 (brown). Figure format as for Fig. 5.

lower density of tie points for 984 and slight differences in the sedimentary environment.

Finally, we also compute the spectrum for the global 0–800 ka relative paleointensity stack of Guyodo and Valet (1999), as it is of interest to compare this with the spectra obtained from individual locations. The global stack is reported at 1 kyr intervals, which we use as our sampling interval in the spectral estimation, although the work of McMillan et al. (2004) makes it clear that the resolution is much less. No scaling is applied to this record since we prefer to preserve the mean VADM (5.8×10^{22} Am^2) representative of the stack itself. We discuss the spectral content of this stack in the context of our composite spectrum below, noting that the absence of specific periodicities in the stack, in particular those associated with orbital modulations, have been reported previously (Guyodo and Valet, 1999).

3.3. The dipole moment for 0–7 ka

For the final high-frequency piece of the spectrum at periods from 1 kyr to 100 years we use the dipole moment from a continuous time-varying geomagnetic field model, CALS7K.2, that spans the time interval 0–7 ka. The model, described in some detail in Korte and Constable (2005), is derived from an extensive set of paleomagnetic observations drawn from globally distributed archeomagnetic and lake sediment studies (Korte et al., 2005). Although the global data distribution is far from uniform, and particularly sparse in the southern hemisphere, the estimate for the dipole moment reflects the longest wavelength field structure and is quite robust. The time-varying model indicates the importance of using the actual dipole moment, rather than some proxy as we have done over longer time intervals. The temporal resolution of the model is no better than 100 years, reflecting the quality and internal consistency of the dating, which in general is better for the archeomagnetic data than for the lake sediments most of which are dated by ^{14}C. Non-dipole field contributions are quite significant at periods of 100–1000 years in this model. Fortunately, we can reject the non-dipole contribution here, but it is worth noting that we might expect them to be present at longer periods too. No scaling was necessary for this part of the dipole spectrum since authors used absolute paleointensity data in generating the model.

3.4. A composite spectrum

The spectra derived from the geomagnetic polarity time scale, marine sedimentary records and a global 0–7 ka model span over six orders of magnitude in frequency (Table 2). For each spectrum, the longest period is determined by the record length, and the shortest period (or Nyquist frequency) by the sampling interval. There is considerable overlap in the frequency bands among different spectra, motivating the construction of a composite spectrum. We do this as follows. For each individual spectrum the lowest frequency (f_{lp}, Table 2) we retain corresponds to periods that are 1/4--1/10 the length of the time series (i.e. the longest period spectral estimates are obtained from at least 4 to 10 cycles in the original time series). The rationale for the highest frequency retained (f_{sp}, Table 2) is record-dependent. For the magnetostratigraphic record, Fig. 4 shows that the spectral estimates fall off rapidly at periods shorter than about 100 kyr, as might be expected given the length of the shortest stable polarity intervals. We cut this spectrum at periods of $10 Myr^{-1}$. Data contributing to VM93, 983 and 984 are obtained by U-channel measurements

Table 2
f_L (f_N)—low (high) frequency limit of individual spectrum based on record determined by the record length and the Nyquist frequency respectively

Record	f_L (Myr^{-1})	f_N (Myr^{-1})	f_{lp} (Myr^{-1})	f_{sp} (Myr^{-1})
Magstrat	0.00625	250	0.025	10
522	0.19	125	1	100
VM93	0.25	250	1.25	150
983	1	5000	10	2500
984	2	5000	10	2500
Sint-800	1.25	500	5	300
CALS7K.2	143	50000	1000	10000

f_{lp}(f_{sp})—low (high) frequency cut-offs applied to individual spectrum to construct the composite.

using pass-through cryogenic magnetometers. The response function of the magnetometers has a peak width at half maximum of 4–5 cm (Weeks et al., 1993) and is likely to smooth the measured record on a length scale about twice as long. For cores 983 and 984, 4 cm averaging reduces the temporal resolution in the records to about 0.4 and 0.3 kyr, respectively, and so we retain only frequencies below 2500Myr^{-1}. For 522, Fig. 5 shows noise in the spectral estimates at frequencies above 100Myr^{-1}, so we retain spectral estimates at frequencies below this cut-off. For VM93, the dip in the spectrum at about 160Myr^{-1} corresponds to larger sampling intervals near the lower end of the section. Because of the variable sampling interval down this core and corresponding variations in sedimentation rate, we retain frequencies below a cut-off of 150Myr^{-1}. For Sint-800 we retain spectral estimates at frequencies below 300Myr^{-1}, because of poor coherence among the contributing records at higher frequencies (McMillan et al., 2004). CALS7K.2 is reported in 10 year intervals, although as mentioned, the real temporal resolution of the model is no better than 100 years, determining our short period cut-off at 10^4 Myr^{-1}.

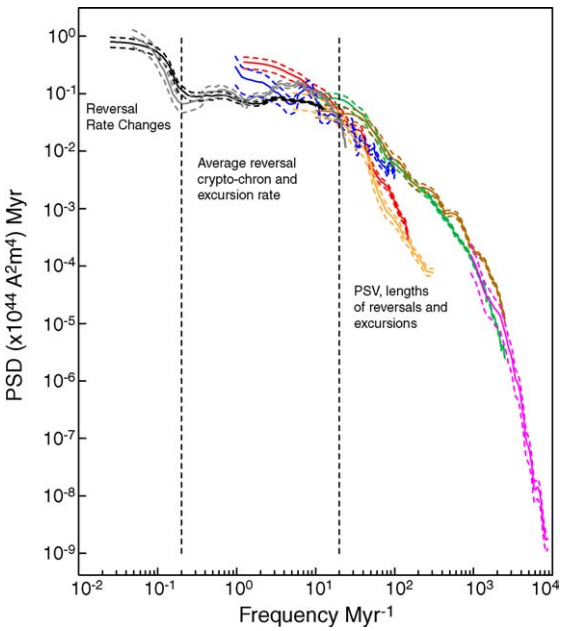

Fig. 7. Composite spectrum: 0–160 Ma reversal record, CK95 (black), 0–83 Ma reversal record including cryptochrons, CK95cc (gray), 522 (blue), VM93 (red), 983 (green), 984 (brown), Sint-800 (orange), and CALS7K.2 (pink).

The composite spectrum is shown in Fig. 7. Overlapping frequency bands among the contributing spectra are 1–10 Myr^{-1} for the CK95 reversal and CK95cc cryptochron records with VM93 and 522, 10–100 Myr^{-1} of VM93 and 522 with 983, 984 and Sint-800, and 1000–2500 Myr^{-1} of 983 and 984 with CALS7K. As noted in Section 3.1.2 there remains an ambiguity about the choice of δ which determines the power in the magnetostratigraphic spectrum. Our choice of $\delta = 30$ kyr means that the magnetostratigraphic spectrum overlaps with those from 522 to 983 in the 1–10 Myr^{-1} frequency band, although it generally appears flatter than the sediment records in this range.

4. Discussion and conclusions

There is a substantial level of agreement among the independently estimated pieces of the dipole moment spectrum. We consider this remarkable in itself. We divide the spectrum into three regions roughly delineated by the dashed lines on Fig. 7. These reflect common perceptions about the time scales for various core processes.

Below 0.02 Myr^{-1} the spectrum is controlled by changes in long term reversal rate. There is substantial power in this range, but it is poorly constrained because of non-stationarity in the reversal rate changes. Between 0.02 and 10 Myr^{-1} the 0–160 Ma magnetostratigraphic spectrum from CK95 is essentially flat, and reflects the average reversal rate during this interval of about 1.8 Myr^{-1}. In this frequency band there is overlap with the intervals covered by 522 and VM93. There are some differences among the estimates which might in part be attributable to the differing average reversal rates in the

time intervals used. The average rate of decay with frequency for 522 and VM93 is quite gentle with a slope that appears to be shallower than f^{-1}, but still significant in comparison with the magnetostratigraphic spectrum. The differences might also be a reflection of long term paleointensity variations associated with different reversal rates. This could perhaps be clarified with a much longer intensity record from sediments. The 0–83 Ma CK95cc cryptochron spectrum is rather similar to that for 522, although the structure introduced by the cryptochrons is broader than the bump at the cryptochron frequency previously identified in the 522 record. It has been debated for some time (Cande and Kent, 1992, 1995), whether the cryptochrons found in the marine magnetic anomaly records are very short polarity intervals, excursions, or large fluctuations in paleointensity. The agreement between the 522 and CK95cc spectra lends support to the idea that they can be any of these, and leads one to suspect that the same kind of physical process might be responsible for all three. This would reinforce the idea that there is nothing special about excursions and reversals, they are simply part of the continuum of observed geomagnetic field behavior. Such a view is compatible with studies of geomagnetic reversals generated in numerical dynamo simulations (Coe et al., 2000; McMillan et al., 2001). A question that arises is whether there is an upper limit to the amount of excursional behavior that can be sustained by the field, or equivalently to the effective reversal rate. Higher rates in the real field require more energy in the poloidal part of the field at high frequencies and would tend to decrease the slope of the spectrum. In Fig. 7 we draw a limit on the excursion rate with the dashed line at 20 Myr^{-1}, but this is an entirely artificial construct. The spectrum does not appear to have a sharp change in slope in this region, but changes gradually into the behavior seen at higher frequencies. In the VM93 record which contains a number of excursions, there is no sign of a peak associated with reversal or excursion rate, just a continuum of field variation between 1 and 10Myr^{-1}. This reflects the long period sawtooth characteristic of the intensity variations which has been discussed elsewhere (Valet and Meynadier, 1993; McFadden and Merrill, 1997).

There is some disagreement among the marine sediment spectra from different records between about 30 Myr^{-1} (30 kyr) and 200 Myr^{-1} (5 kyr). While 522, and the two spectra from Garder drift are quite consistent, the VM93 and Sint-800 estimates show substantially less power in the secular variation. We might expect this to be the case for Sint-800, which is derived from the average of a stack of relative paleointensity records of variable length, and sedimentation rate. The age correlations among these records are typically based on SPECMAP (Martinson et al., 1987) so in addition to averaging of non-dipole field effects, we would expect a loss of temporal resolution from combining globally distributed sites. McMillan et al. (2002, 2004) expect the coherence of any global dipolar signal to be substantially attenuated at periods shorter than about 20 kyr, and this is compatible with what is seen in the accelerated spectral fall-off in Fig. 7.

It is less obvious why VM93 should be in such good agreement with Sint-800 over this frequency band rather than falling in the same range as the other records. One would expect a single record to show more variance than the average. We consider two possibilities: (1) the sedimentation process, remanence acquisition, and/or subsequent remagnetization may smooth the record; (2) variations in VADM records that result from geographically variable non-dipole field contributions. The average sedimentation rate for VM93 is about a factor of five less than for 983 (Table 1), which could well play a role in this process. This is supported by analyses of the 1 Myr segments which show more power associated with the higher accumulation rate part of the record. However, the 522 record has an even lower accumulation rate but higher power than VM93 at the high frequency limit. It has been suggested (Kok and Tauxe, 1996; Mazaud, 1996) and rebutted (Meynadier and Valet, 1996) that viscous or postdepositional realignment of remagnetization may be responsible for the sawtooth intensity variations, and it is perhaps possible that this could generate broadband attenuation of the spectral content. Geographically variable non-dipole effects cannot be ruled out as a contributing factor, but the difference between VM93 and the Garder Drift estimates is about one and one half orders of magnitude, which seems excessively large. Furthermore the overlap of the Garder drift and CALS7K.2 estimates would argue for reliability of Garder 983 and 984 records, since CALS7K.2 is the most reliable estimate of the dipole moment that we have, and does not rely on auxiliary calibration. Beyond 1000 Myr^{-1} the Garder drift spectra also drop off steeply. At the highest frequencies there is a very steep falloff in the dipole spectrum for CALS7K.2, suggesting very little power in dipole variations at this frequency. This picture can be expected to change somewhat as better spherical harmonic models become available for the 0–50 ka time intervals.

We conclude with a summary of the results we consider reliable. The empirical estimates currently available do not indicate any distinction in spectral behavior that allows separation of excursional and transitional field behavior from what might be called

normal secular variation, although there does seem to be a characteristic spectral signature associated with the recurrence time of cryptochrons during the Oligocene: this signature is also seen in the magnetostratigraphic record when cryptochrons are included in the analysis and may reflect short polarity intervals, excursions or just large intensity variations. We consider it likely that these can all be generated by the same kind of process.

Each kind of spectral estimate will be reliable over a restricted range of frequencies. The CK95 reversal spectrum lacks the energy associated with paleosecular variation, but provides a good representation for long period changes associated with average reversal rate and changes in that rate (frequency range 10^{-2} to 1Myr^{-1}). Between 1 and 7Myr^{-1} CK95 may not resolve cryptochrons and almost certainly underestimates power, but CK95cc does a better job. Above frequencies of about 7Myr^{-1} both CK95 and CK95cc fall off rapidly and severely underestimate the spectral power. VM93 and 522 overlap with CK95 and CK95cc and should provide the most reliable spectral estimates in the frequency range 1–70 Myr^{-1}. Although VM93 has a Nyquist frequency of 500 Myr^{-1} we infer that the low sedimentation rate combined with other factors contributes to an attenuated PSV record compared with that obtained from the Garder drift sediments. The upper envelope of the overlapping spectra will provide the most reliable paleomagnetic power spectrum.

The spectrum cannot be described by a simple power law dependency on frequency as has been advocated by some earlier studies. If further paleomagnetic investigations of longer intensity records reveal that between frequencies of 0.2 and 20 Myr^{-1} the spectrum is essentially flat, then this would provide the first visible evidence of a separation in the time scales of physical processes influencing changes in reversal rate from the actual reversal process itself. Then it will also be possible to derive estimates of how long is needed to determine the time-averaged field associated with an essentially constant reversal rate. There is substantial scope for improvement of the spectra presented here. Many more relative paleointensity data are now available, particularly for the 0–1 Ma time period, and we plan a systematic study of geographic variations among these records, with a view to clarifying the spectral structure between 30 and 1000 Myr^{-1}.

Acknowledgments

This work could not have been done without the multitaper spectral code (PSD) and the ever-useful PLOTXY used to generate all the figures. Bob Parker is the author of both, and we are grateful for his continued interest in developing and maintaining them. Thanks also to Jim Channell for sending us the Garder Drift data. Support for this work came from NSF grant EAR 0337712. We thank reviewers Charles Barton and Frederik Simons for comments which led us to uncover an egregious error in our initial analyses of the reversal record.

References

Akima, H., 1970. A new method of interpolation and smooth curve fitting based on local procedures. J. Assoc. Comp. Mach. 17, 589–602.

Barton, C.E., 1982. Spectral analysis of palaeomagnetic time series and the geomagnetic spectrum. Phil. Trans. R. Soc. Lond. A306, 203–209.

Barton, C.E., 1983. Analysis of paleomagnetic time series—techniques and applications. Geophys. Surv. 5, 335–368.

Barton, C.E., McElhinny, M.W., 1982. Time series analysis of the 10000 yr geomagnetic secular variation record from SE Australia. Geophys. J. R. Astr. Soc. 68, 709–724.

Blackman, R.B., Tukey, J.W., 1958. The Measurement of Power Spectra From the Point of View of Communication Engineering. Dover Publications, New York.

Bouligand, C., Hulot, G., Khokhlov, A., Glatzmaier, G.A., 2005. Statistical paleomagnetic field modelling and dynamo numerical simulation. Geophys. J. Int. 161, 603–626.

Burg, J.P., 1967. Maximum entropy spectral analysis. Proceedings of the 37th Annual International Meeting of Society on Exploration Geophysics. Oklahoma City.

Cande, S.C., Kent, D.V., 1992. Ultrahigh resolution marine magnetic anomaly profiles: a record of continuous paleointensity variations. J. Geophys. Res. 97 15, 15075–15083.

Cande, S.C., Kent, D.V., 1995. Revised calibration of the geomagnetic polarity timescale for the late Cretaceous and Cenozoic. J. Geophys. Res. 100, 6093–6095.

Channell, J.E.T., 1999. Geomagnetic paleointensity and directional secular variation at Ocean Drilling Program (ODP) Site 984 (Bjorn Drift) since 500 ka; comparisons with ODP Site 983 (Gardar Drift). J. Geophys. Res. B 104, 22937–22951.

Channell, J.E.T., Hodell, D.A., McManus, J., Lehman, B., 1998. Orbital modulation of geomagnetic paleointensity. Nature 394, 464–468.

Coe, R.S., Hongre, L., Glatzmaier, G.A., 2000. An examination of simulated geomagnetic reversals from a palaeomagnetic perspective. Phil. Trans. R. Soc. Lond. Ser. A 358, 1141–1170.

Constable, C., 2000. On rates of occurrence of geomagnetic reversals. Phys. Earth Planet. Int. 118, 181–193.

Constable, C.G., 2003. Geomagnetic reversals: rates, timescales, preferred paths, statistical models, and simulations. In: Jones, Christopher A., Soward, Andrew M., Zhang, Keke (Eds.), Earth's Core and Lower Mantle. Taylor and Francis, London 77–99.

Constable, C.G., Tauxe, L., Parker, R.L., 1998. Analysis of 11 Myr of geomagnetic intensity variation. J. Geophys. Res. 103, 17735–17748.

Courtillot, V., Le Mouël, J.-L., 1988. Time variations of the Earth's magnetic field: from daily to secular. Ann. Rev. Earth Planet. Sci. 16, 389–476.

Cox, A.V., 1969. Geomagnetic reversals. Science 163, 237–245.
Denham, C.R., 1975. Spectral analysis of paleomagnetic time series. J. Geophys. Res. 80, 1897–1901.
Guyodo, Y., Valet, J.P., 1999. Global changes in geomagnetic intensity during the past 800 thousand years. Nature 399, 249–252.
Guyodo, Y., Gaillot, P., Channell, J.E.T., 2000. Wavelet analysis of relative geomagnetic paleointensity at ODP Site 983. Earth Planet. Sci. Lett. 184, 109–123.
Harland, W.B., Armstrong, R.L., Cox, A.V., Craig, L.E., Smith, A.G., Smith, D.G., 1990. A Geological Time Scale 1989. Cambridge University Press, Cambridge.
Hartl, P.D., Tauxe, L., Constable, C., 1993. Early oligocene geomagnetic field behavior from DSDP Site 522. J. Geophys. Res. 98, 19649–19665.
Kok, Y., Tauxe, L., 1996. Sawtooth pattern of relative paleointensity records and cumulative viscous remanence. Earth Planet. Sci. Lett. 137, 95–99.
Kono, M., Roberts, P.H., 2002. Recent geodynamo simulations and observations of the geomagnetic field. Rev. Geophys. 40, 1013 doi:10.1029/2000RG000102.
Korte, M., Genevey, A., Constable, C.G., Frank, U., Schnepp, E., 2005. Continuous geomagnetic models for the past 7 millennia. I. A new global data compilation. Geochem. Geophys. Geosyst. 6 2, Q02H15 doi:10.1029/2004GC000800.
Korte, M., Constable, C.G., 2005. Continuous geomagnetic models for the past 7 millennia. II. CALS7K. Geochem. Geophys. Geosyst. 6 2, Q02H16 doi:10.1029/2004GC000801.
Martinson, D.G., Pisias, N., Hayes, J.D., Imbrie, J., Moore Jr., T.C., Shackleton, N.J., 1987. Age dating and orbital theory of ice ages: development of a high resolution 0–300,000 year chronostratigraphy. Quat. Res. 27, 1–29.
Mazaud, A., 1996. Sawtooth variation in magnetic profiles and delayed acquisition of magnetization in deep sea cores. Earth Planet. Sci. Lett. 139, 379–386.
McFadden, P.L., Merrill, R.T., 1997. Sawtooth paleointensity and reversals of the geomagnetic field. Phys. Earth Planet. Int. 103, 247–252.
McMillan, D.G., Constable, C.G., Parker, R.L., Glatzmaier, G.A., 2001. A statistical appraisal of magnetic fields of geodynamo models. Geochem. Geophys. Geosyst. 2 doi:10.129/2000GC000130, 2001.
McMillan, D.G., Constable, C.G., Parker, R.L., 2002. Limitations on stratigraphic analyses due to incomplete age control and their relevance to sedimentary paleomagnetism. Earth Planet. Sci. Lett. 201, 509–523.
McMillan, D.G., Constable, C.G., Parker, R.L., 2004. Assessing the dipolar signal in stacked paleointensity records using a statistical error model and geodynamo simulations. Phys. Earth Planet. Int. 145, 37–54.
Merrill, R.T., McElhinny, M.W., McFadden, P.L., 1996. The Magnetic Field of the Earth: Paleomagnetism, the Core and The Deep Mantle. Academic Press, San Diego, California.
Meynadier, L., Valet, J.-P., 1996. Post-depositional realignment of magnetic grains and asymmetrical saw-tooth patterns of magnetization intensityě. Earth Planet. Sci. Lett. 140, 123–132.
Paillard, D., Labeyrie, L., Yiou, P., 1996. Macintosh program performs time-series analysis. Eos. Transactions, vol. 77. American Geophysical Union p. 379, http://www.agu.org.eos_elec.
Percival, D.B., Walden, A.T., 1993. Spectral Analysis for Physical Applications: Multi-taper and Conventional Univariate Techniques. Cambridge University Press, Cambridge, England.
Prévot, M., Derder, M.E., McWilliams, M., Thompson, J., 1990. Intensity of the Earth's magnetic field: evidence for a Mesozoic dipole low. Earth Planet. Sci. Lett. 97, 129–139.
Riedel, K., Sidorenko, A., 1995. Minimum bias multiple taper spectral estimation. IEEE Trans. Sig. Process. 43, 188–195.
Roberts, A.P., Winkelhofer, M., Liang, W-T., Horng, C.-S., 2003. Testing the hypothesis of orbital (eccentricity) influence on Earth's magnetic field. Earth Planet. Sci. Lett. 216, 187–192.
Schuster, A., 1898. On the investigation of hidden periodicities with application to a supposed 26 day period of meteorological phenomena. Terr. Magn. 3, 13–41.
Shackleton, N.J., Crowhurst, S., Hagelberg, T., Pisias, N.G., Schneider, D.A., 1995. A new Late Neogene time scale: application to leg 138 sites. Proceedings of the Ocean Drilling Program, Scientific Results, vol. 138. 73–97.
Tauxe, L., 2005. Long term trends in paleointensity: the contribution of DSDP/ODP submarine basaltic glass collections. Phys. Earth. Planet. Int.
Tauxe, L., Hartl, P., 1997. 11 million years of geomagnetic field behavior. Geophys. J. Int. 128, 217–229.
Thomson, D.J., 1982. Spectrum estimation and harmonic analysis. IEEE Proc. 70, 1055–1096.
Valet, J.-P., Meynadier, L., 1993. Geomagnetic field intensity and reversals during the last four million years. Nature 366, 234–238.
Weeks, R., Laj, C., Endignoux, L., Mazaud, A., Labeyrie, L., Roberts, A., Kissel, C., Blanchard, E., 1993. Improvements in long-core measurement techniques: applications in palaeomagnetism and palaeoceanography. Geophys. J. Int. 114, 651–662.
Wollin, G., Ryan, W.B.F., Ericson, D.B., 1978. Climatic changes, magnetic intensity variations and fluctuations of the eccentricity of the Earth's orbit during the past 2,000,000 years and a mechanism which may be responsible for the relationship. Earth Planet. Sci. Lett. 41, 395–397.
Yamazaki, T., Oda, H., 2002. Orbital influence on Earth's magnetic field: 100,000 year periodicity in inclination. Science 295, 2435–2438.